ISBN: 978-3-95450-201-1 doi:10.18429/JACoW-IBIC2018-MOPA17

MOMENTUM COMPACTION MEASUREMENT USING SYNCHROTRON RADIATION

L. Torino*, N. Carmignani, A. Franchi, ESRF, 38000 Grenoble, France

Abstract

The momentum compaction factor of a storage ring can be obtained by measuring how the beam energy changes with the RF frequency. Direct measurement of the beam energy can be difficult, long or even not possible with acceptable accuracy and precision in some machines such as ESRF. Since the energy spectrum of the Synchrotron Radiation (SR) depends on the beam energy, it is indeed possible to relate the variation of the beam energy with a variation of the produced SR flux. In this proceeding, we will present how we obtain a measurement of the momentum compaction using this dependence.

INTRODUCTION

The variation of path length (L) with momentum (p) is determined by the momentum compaction factor (α_c) defined by:

$$\frac{\Delta L}{L} = \alpha_c \frac{\Delta p}{p}, \tag{1}$$

with $\frac{\Delta p}{p} \ll 1$ [1].

Assuming that particles are ultra-relativistic ($v \simeq c$, where c is the speed of light), ΔL is directly related with RF frequency variation, Δf_{RF}:

$$\frac{\Delta L}{L} = -\frac{\Delta f_{\mathrm{RF}}}{f_{\mathrm{RF}}}, \tag{2}$$

while the measurement of the momentum variation leads to some difficulties.

Using the same assumption, the momentum p can be approximated to the beam energy E and:

$$\frac{\Delta p}{p} \simeq \frac{\Delta E}{E}. \tag{3}$$

Substituting Eq. (2) and Eq. (3) in Eq. (1) one obtains:

$$\frac{\Delta E}{E} = -\alpha_c \frac{\Delta f_{RF}}{f_{RF}}. \tag{4}$$

In high-energy accelerators, and in particular in synchrotron light sources, the most accurate way to measure the energy is via the "spin depolarization" [2–4]. Unfortunately this technique cannot be used in all the machines depending on the complexity of the lattice [5]. Moreover the whole measuring process is time consuming.

On the other hand the momentum compaction factor measurement can be obtained by measuring the relative energy variation $\frac{\Delta E}{E}$. A method to obtain this quantity has been proposed based on the observation of the shift of the spectral peaks produced by an undulator [6, 7]. The observation is also quite complex and time consuming since it involves the access to a full beamline to measure the full SR spectrum.

The new technique to obtain α_c, proposed in this proceeding, is based on the measure of $\frac{\Delta E}{E}$ by using the relation between the produced SR flux and the beam energy.

MOMENTUM COMPACTION AND SYNCHROTRON RADIATION

The total SR power emitted by a charged particle with unit charge in a bending magnet is given by:

$$P_0 = \frac{8}{3}\pi\varepsilon_0 r_0^2 c^3 \frac{E^2 B^2}{(mc^2)^2}, \tag{5}$$

where ε_0 is the vacuum permittivity, r_0 is the classical electron radius, m is the rest mass of the particle, and B is the magnetic field [8]. From Eq. (5), it is clear that P_0 depends on the beam energy E, however a direct measurement of the total SR power is not possible.

A good observable is instead the intensity of the hard portion of the SR, which depends on P_0. The flux produced by an electron beam with an energy of 6.04 GeV, and one produced by increasing the beam energy of 5% are presented in Fig. 1: the fluxes start to be consistently different for photon energies larger than 100 keV.

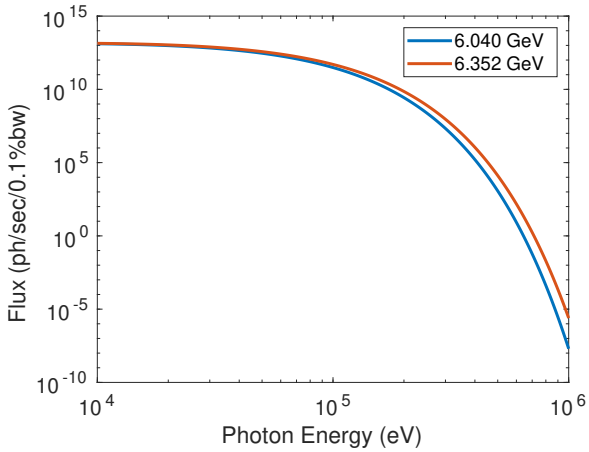

Figure 1: Photon flux produced by a beam of 6.04 GeV (blue) and the one produced by increasing the beam energy of 5% (orange).

High-energy photons can be selected by filtering the SR using an absorber, and detected by using, for example, a scintillator and a CCD camera.

The total intensity of the signal hence depends on the beam energy and although it is not possible to relate it with

* laura.torino@esrf.fr

Content from this work may be used under the terms of the CC BY 3.0 licence (© 2018). Any distribution of this work must maintain attribution to the author(s), title of the work, publisher, and DOI.

ISBN: 978-3-95450-201-1 doi:10.18429/JACoW-IBIC2018-MOPA17

the absolute value, any relative energy variation can be detected and quantified from the relative change of the intensity detected by the CCD camera [9]. Figure 2 shows an example of intensity variation when performing a RF step of 100 Hz.

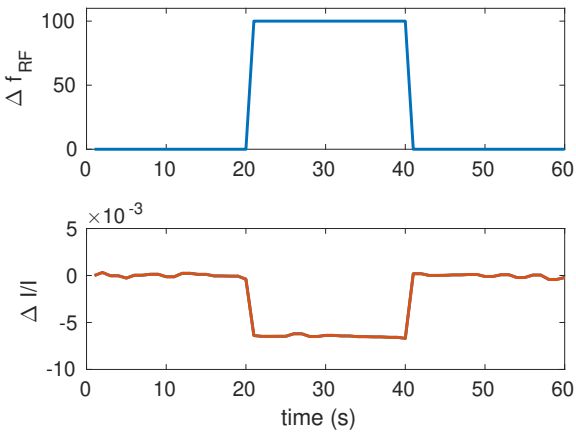

Figure 2: Example of RF step (top) inducing a SR intensity variation (bottom).

The relation between the electron beam energy and the SR intensity depends on the x-rays spectrum and on the radiation optical path.

In order to measure the momentum compaction factor, the idea is to record the SR intensity variation for different RF frequency steps. The relative change of SR intensity is then converted into electron beam energy variation using a coefficient given by the simulation of the SR passing through the optical path. Fitting the data with Eq. (4), the momentum compaction factor is obtained.

CALCULATION OF THE CONVERSION COEFFICIENT

The software used to simulate the SR and the optical path is the X-ray Oriented Programs (XOP) [10].

XOP produces the emitted SR spectrum for a given beam. The parameters required are the machine radius, or equivalently the magnetic field, and the beam energy. Other parameters, such as the beam current, are not relevant for the scope of these simulations, since they are cancelled out when evaluating the relative variation of the SR intensity.

The same software also produces the transmittance and absorption curve of different material for a defined thickness, as a function of the photon energy spectrum. These curves are used to simulate the x-rays optical path.

A Python script has been written to propagate the x-ray spectrum through the different materials using the transmission curve, and to estimate the number of photons absorbed in the scintillator at the end of the optical path.

The photon absorbed are converted into visible light by the scintillator. The signal produced by the material is linear with the x-ray photon energy absorbed and the linear coefficient is provided by the scintillator manufacturer.

The whole process can be translated in formula as:

$$I(E) = \int_0^\infty f(E_p) \times T_{\mathrm{OP}}(E_p) \times A_S(E_p) \times C_s \times E_p \, \mathrm{d}E_p; \quad (6)$$

where $I(E)$ is the intensity observed on the CCD and depends on the beam energy E, and E_p is the energy spectrum of the SR produced, $f(E_p)$ is the initial flux at a given beam energy, $T_{\mathrm{OP}}(E_p)$ is the transmission of the optical path, $A_S(E_p)$ is the absorption of the scintillator, and C_s is the scintillator linear coefficient.

The simulation has to be repeated for several energies in the range of the expected energy excursion. The final output is the dependence of the observed relative change of the SR intensity ($\frac{\Delta I}{I}$) from the generated beam energy variation ($\frac{\Delta E}{E}$).

EXPERIMENTAL SETUP AND PREPARATION

Experiments were performed at the storage ring of the European Synchrotron Radiation Facility (ESRF). The machine parameters are presented in Table 1.

Table 1: ESRF Machine Parameters

Parameter	Unit	Value
Energy	GeV	6.04
RF frequency	MHz	352
Horizontal Emittance	nm	4
Vertical Emittance	pm	4
Magnetic Field	T	0.86

SR coming from the first bending magnet in cell 7 is extracted through an absorber made out of 28 mm of copper, and through a 2 mm aluminum extraction window. The absorber is a simple, solid, copper parallelepiped designed for non-destructive halo monitoring [11].

X-rays are converted into visible light by 6 mm of Cadmium-Tungstate scintillator ($CdWO_4$, $C_s \simeq 13$ ph/keV [12]), and imaged through an objective to a CCD camera.

A sketch of the experimental setup is presented in Fig. 3, and Fig. 4 shows an example of the image obtained at the CCD.

Coefficient Calculation

The coefficient K relating the relative SR intensity variation with the relative electron beam energy change,

$$\frac{\Delta I}{I} = K \frac{\Delta E}{E}, \quad (7)$$

has been found using XOP, as explained in the previous section.

The simulated SR spectrum (flux) before and after the optical path is presented in Fig. 5.

To calculate the conversion coefficient, the SR spectrum has been generated for beam energies corresponding to an

Content from this work may be used under the terms of the CC BY 3.0 licence (© 2018). Any distribution of this work must maintain attribution to the author(s), title of the work, publisher, and DOI.

ISBN: 978-3-95450-201-1 doi:10.18429/JACoW-IBIC2018-MOPA17

Content from this work may be used under the terms of the CC BY 3.0 licence (© 2018). Any distribution of this work must maintain attribution to the author(s), title of the work, publisher, and DOI.

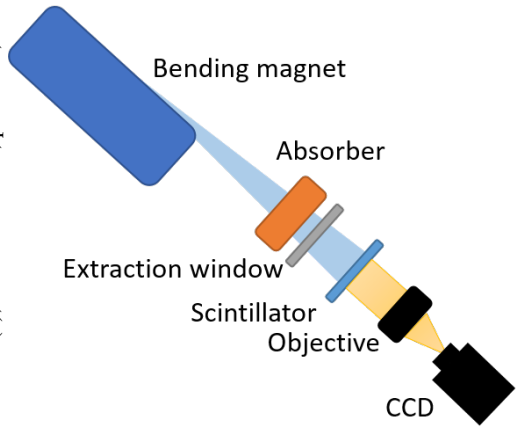

Figure 3: Momentum compaction experimental setup: SR produced by a bending magnets is filtered by a copper absorber and extracted through an extraction window. The radiation is then converted into visible light by a scintillator and imaged onto a CCD camera by an objective.

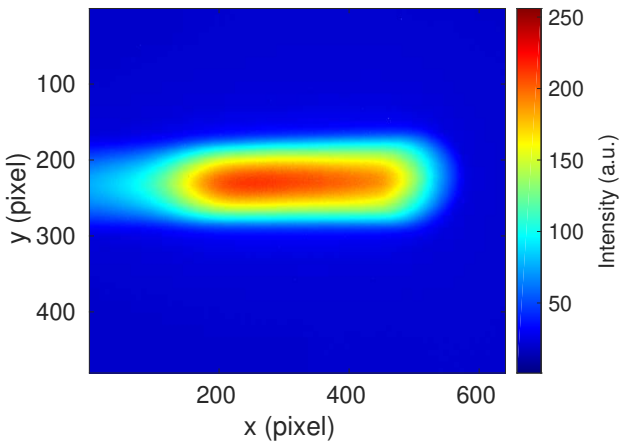

Figure 4: Image obtained at the CCD location.

RF excursion of ±40 Hz (≃ ±10 MeV). The spectra are propagated through the optical path, and the expected intensity has been calculated according to Eq. (6). The variation of intensity is given by:

$$\frac{\Delta I}{I} = \frac{I(E) - I(E_0)}{I(E_0)};$$

where $I(E_0)$ is the intensity obtained at $E_0 = 6.04$ GeV and $I(E)$ is the intensity for a given beam energy, E.

The plot of the correspondence between electron beam energy and SR intensity is presented in Fig. 6. From the linear fit of this curve, the conversion coefficient K is inferred. The result is:

$$\frac{\Delta I}{I} = 17.16 \times \frac{\Delta E}{E}. \quad (8)$$

Calibration Varying the Magnetic Field

In order to verify the accuracy of the optical path model, an independent, experimental, beam-based calibration has

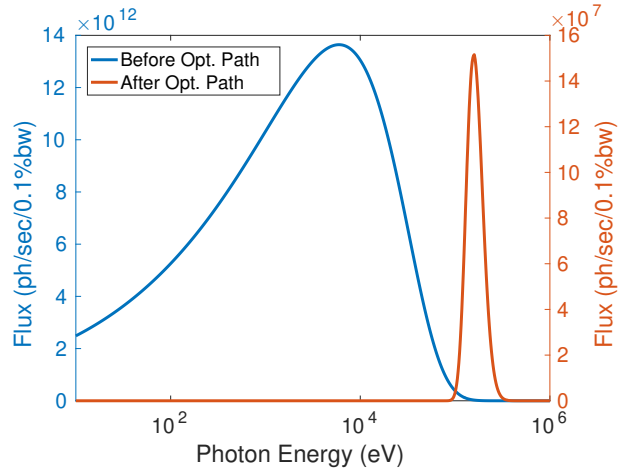

Figure 5: Energy spectrum of the produced SR at 6.04 GeV before the optical path (blue) and at the end of it (orange). Note the different scales on the right and left vertical axis.

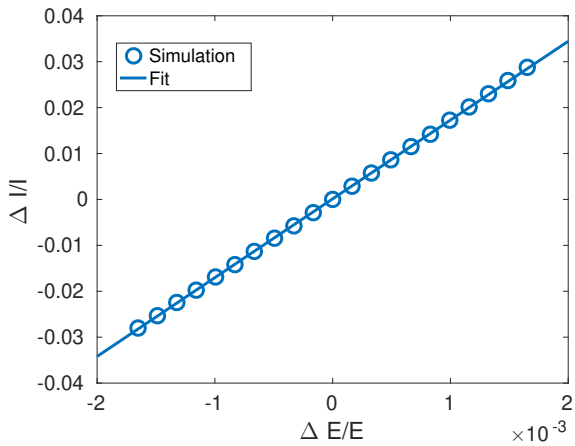

Figure 6: Relation between the electron beam energy and the SR intensity variation. Dots are obtained by XOP simulations, whereas the line is computed by a linear fit.

been performed by varying the magnetic field of all the bending magnets in the storage ring, and consequently the beam energy, maintaining the orbit length constant:

$$\rho \propto \frac{E}{B}, \quad (9)$$

being ρ is the machine bending radius.

For different values of B (and hence of E, since $\frac{\Delta B}{B} = \frac{\Delta E}{E}$), the produced SR intensity has been recorded. The same experiment has been simulated using XOP.

The measured and the simulated intensity variations have been found to be in good agreement: results are shown in Fig. 7.

RESULTS

Momentum compaction factor measurements have been performed three different times, in 2017. In general, the RF has been varied within a ±40 Hz range, which corresponds

ISBN: 978-3-95450-201-1 doi:10.18429/JACoW-IBIC2018-MOPA17

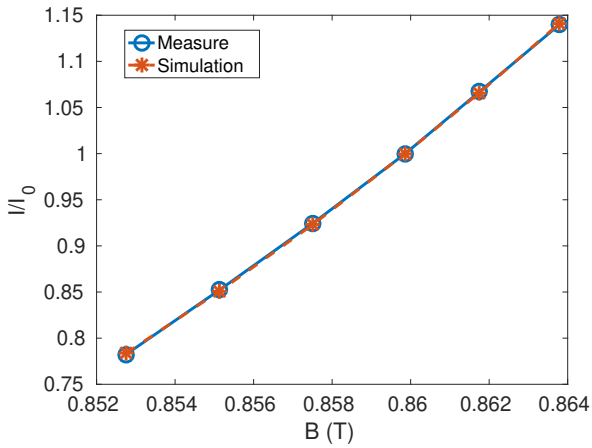

Figure 7: SR normalized intensity Vs dipole field B at a fixed orbit. Measured data in blue, simulation in orange.

to a relative change of beam energy of about 6.4×10^{-4}. Ten images per frequency has been saved, the intensity of each image was normalized to the beam current to account for possible beam losses during the frequency scan.

In order to avoid effects related with the CCD camera noise drift, the RF has been varied in an "alternate way", as depicted in Fig. 8.

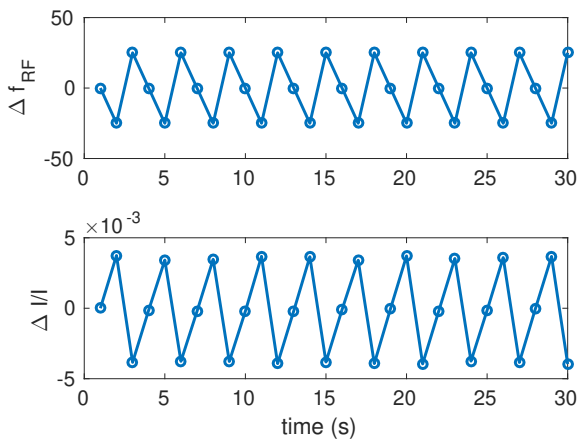

Figure 8: Set RF frequency shifts (top) and measured SR intensity variation (bottom). The "alternate RF variation" consists on the repeated sequence: f_{RF}, $f_{RF} - \Delta f_{RF}$, $f_{RF} + \Delta f_{RF}$.

To minimize the effect of the background noise, images are averaged and an image taken with no beam and same CCD settings is subtracted.

A suitable Region Of Interest (ROI) has been selected and the integral of the ROI has been used to calculate $\frac{\Delta I}{I}$. The energy variation $\frac{\Delta E}{E}$ is calculated by inverting Eq. (8).

Results are then plotted as a function of the relative variation of the RF frequency $\frac{\Delta f_{RF}}{f_{RF}}$ and fitted using Eq. (4): the coefficient of the fit provides the machine momentum compaction factor. An example is presented in Fig. 9. The obtained result is:

$$\alpha_c = (1.814 \pm 0.004) \times 10^{-4}, \quad (10)$$

which is compatible with the one computed from the electron beam optics model obtained from the analysis of the Orbit Response Matrix (ORM) $\alpha_{c,M} = 1.8172 \times 10^{-4}$.

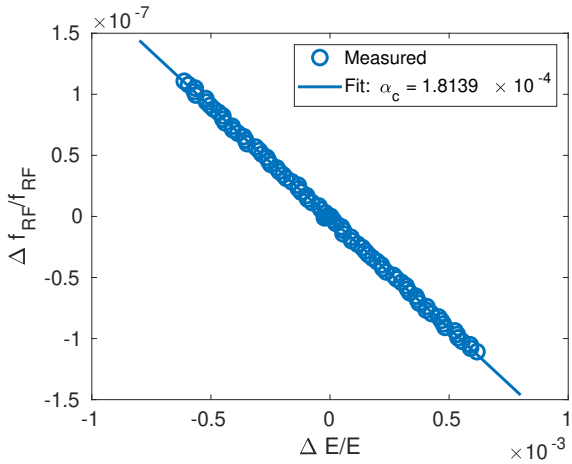

Figure 9: Example of momentum compaction factor measurement: $\frac{\Delta E}{E}$ dots are calculated from the SR intensity measurements, whereas the solid line represents the fit from whose slope the momentum compaction is inferred.

Table 2 presents all the measurements of the momentum compaction factor obtained using this techniques over several months and the results inferred from the ORM.

Table 2: Results of momentum compaction factor measurements and from the ORM.

$\alpha_c \times 10^{-4}$	$\alpha_{c,M} \times 10^{-4}$
1.814 ± 0.004	1.8172
1.816 ± 0.002	1.833
1.806 ± 0.003	1.8273

CONCLUSION

In this proceeding a new technique to measure the momentum compaction factor based on SR intensity measurements has been proposed. Experimental tests performed at ESRF and their results have been presented proving the precision (better than 10^{-6}) and the reliability of the technique. The relative error on the measurement is in the order of 0.1%.

ACKNOWLEDGMENTS

The authors would like to thank K. B. Scheidt for the main idea, F. Ewald for the help with the technical issues with the CCD cameras, and the ESRF accelerator and source division for the grate job in operating and maintaining the machine.

Content from this work may be used under the terms of the CC BY 3.0 licence (© 2018). Any distribution of this work must maintain attribution to the author(s), title of the work, publisher, and DOI.

ISBN: 978-3-95450-201-1 doi:10.18429/JACoW-IBIC2018-MOPA17

Content from this work may be used under the terms of the CC BY 3.0 licence (© 2018). Any distribution of this work must maintain attribution to the author(s), title of the work, publisher, and DOI.

REFERENCES

[1] H. Wiedemann, *Particle Accelerator Physics I*, Berlin Heidelberg, Springer, 1998. doi:10.1007/978-3-662-03827-7

[2] L. Arnaudon, *et al.*, "Accurate determination of the LEP beam energy by resonant depolarization", *Zeitschrift für Physik C Particles and Fields*, vol. 66, no. 1, pp. 45–62, Mar. 1995. doi:10.1007/BF01496579

[3] J. Zhang *et al.*, "Precise beam energy measurement using resonant spin depolarization in the SOLEIL storage ring", *Nuclear Instruments and Methods in Physics Research Section A: Accelerators, Spectrometers, Detectors and Associated Equipment*, vol. 697, pp. 1–6, 2013. doi:10.1016/j.nima.2012.09.003

[4] A.-S. Müller *et al.*, "Momentum compaction factor and nonlinear dispersion at the ANKA storage ring", in *Proc. EPAC'04*, Lucerne, Switzerland, Jul. 2004, paper WEPLT068, pp. 2005–2007.

[5] N. Carmignani *et al.*, "Modeling and measurement of spin depolarization", in *Proc. IPAC'15*, Geneva, Switzerland, Jun. 2015, pp. 109–112. doi:10.18429/JACoW-IPAC2015-MOPWA013

[6] E. Tarazona and P. Elleaume, "Measurement of the absolute energy and energy spread of the ESRF electron beam using undulator radiation", *Rev. Sci. Instr.*, vol. 67, no. 9, p. 3368, 1996. doi:10.1063/1.1147371

[7] B. Yang *et al.*, "High accuracy momentum compaction measurement for the APS storage ring with undulator radiation", *AIP Conference Proceedings*, vol. 546, no. 1, pp. 234–241, 2000. doi:10.1063/1.1342591

[8] A. Hofmann, "Characteristic of Synchrotron Radiation", in *Proc. CERN Accelerator School, Synchrotron Radiation and Free Electron Lasers*, Chester, UK, Apr. 1989, pp. 115–141, published 1990, and CERN rep. CERN-90-03.

[9] K. B. Scheidt, "Recent developments of novel beam diagnostics at the ESRF", in *Proc. IPAC'13*, Shanghai, China, May 2013, paper TUOCB201, pp. 1143–1145.

[10] X-ray Oriented Programs, http://www.esrf.eu/Instrumentation/software/data-analysis/xop2.4

[11] K. B. Scheidt, "Non destructive vertical halo monitor on the ESRF's 6 GeV electron beam", in *Proc. IBIC'14*, Monterey, CA, USA, Sep. 2014, paper MOCYB1, pp. 2–6.

[12] Saint Gobain, www.crystals.saint-gobain.com